Advance Researches in Civil Engineering
ISSN: 2645-7229, Vol.4, No.4, pages: 55-70

Effect of Hydraulic and Geometrical Parameters of Skimming Wall on Controlling Sediment Entering Lateral Intakes Using Harmony Search Algorithm

Bahador Fatehi-Nobarian [1*], Sadegh Farshidnia [2], Mojtaba Saneie [3]

[1] Assistant Professor, Department of Civil Engineering of Hydraulic Structures, Islamic Azad University,*

Aras Branch, Jolfa, Iran

(b.fatehinobarian@iaut.ac.ir)

[2] Ph.D. of Civil Engineering of Hydraulic Structures -Associate Member of IRCOLD

[3] Associate Professor, Soil Conservation and Watershed Management Research Institute, (SCWMRI), Agricultural Research, Education and Extension, Organization (AREEO), Tehran-Iran

(Date of received: 05/08/2022, Date of accepted: 26/12/2022)

ABSTRACT

In this article, the control over the inlet sediment into the lateral intakes incorporating parallel skimming walls is assessed using harmony search algorithm. The skimming walls are known as the structures constructed in front of the lateral intake and consisted of two plates, one of them is in oblique form and the other one is parallel to the flow. The parallel skimming walls direct the sediments toward the downstream of the main channel by forming a rotational flow, as a result the entry of sediments into the lateral intake is prevented. Using the experimental data obtained in the laboratory and Buckingham's method, the dimensionless parameters were obtained. The parameters were nonlinearly transformed into the relations, in such a way that using harmony search algorithm almost 20,000 optimal points were obtained. In the present research, the relations between the dimensionless parameters were yielded by harmony search algorithm. The results indicate that the optimized maximum and minimum and mean values of C_{S1} for $C_{s1}=\frac{V_1}{D_1^3}$ governing equations is equal to 17%, 31% and 29%, respectively, relative to the observational maximum, minimum and mean values of C_{S1}. For $C_{s2}=\frac{V_2}{D_2^3}$ governing equation, the optimized maximum, minimum and mean values of C_{S2} exhibited error values of 11%, 4% and 31% relative to the observational maximum, minimum and mean value of C_{S2}.

Keywords:

Lateral Intake, Skimming Wall, Sediment Control, Harmony Search Algorithm.

Advance Researches in Civil Engineering
ISSN: 2645-7229, Vol.4, No.4, pages: 55-70

1. Introduction

Intake is defined as a hydraulic structure constructed for water deviation and regulation of the water level. Generally, this structure is used in the water supply networks, irrigation channels, sewage grids and electric plants input section. The flow within a branch of intake is of 3D type and it possesses complexities [1]. Several factors have impact on the conditions of inlet flow into the intake span and the amount of inlet sediment, such as channel type (direct or curved), intake placement location, intake angle, the discharge ratio of main channel to secondary channel, hydraulic conditions of the flow in the main channel, type and grading of the sediment load (bed load or suspended load), flow depth, presence of sill and submerged vanes or other intakes at the upstream, and each of these factors may impose drawbacks and advantages. The skimming walls are newly developed structures which can play an important role in banishing the bed load sediments from the intake span. This structure creates a rotational flow at downstream, whose expansion imposes transverse shear on the riverbed (where high amount of sediment is found) [2]. The vortices at the down edge of the wall, not only rotate but also they go to the downstream along the flow and lead to creation of greater vortices. The vortices are developed close to top of the edge of the wall [3]. Finally, the creation of a relatively deep continuous groove along the main channel length in front of the intake span, directs the sediments toward the downstream, as a result the amount of sediment entering the lateral intake is reduced. In the present research, using experimental instruments and harmony search algorithm, the impact of parallel skimming walls on reducing the inlet sediment into the intake is examined. Figure 1 depicts a plan of channels and parallel skimming walls.

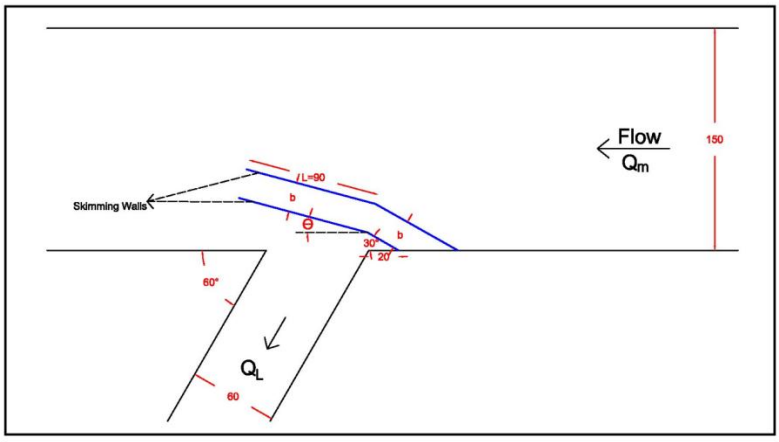

Figure 1. Plan of experimental flume and parallel skimming walls of the present study (all measurements are per cm).

2. Review of literature

Abbasi [4] conducted experimental study on sediment controlling in the lateral intake located in the direct trajectories. They studied the controlling methods of inlet sediment to the lateral intake located in the direct paths, considering two modes, namely, using sill and submerged vanes. They revealed that the sediment entry into the intake in the presence of sill, submerge vanes or absence of any of them, is depended on the dimensionless parameters of flow Froude number, intake discharge and intake angle of channel. Among them, intake discharge plays a major role, and any increase in the intake discharge ratio led to increase in the amount of sediment entering intake. Seyedian and Shafaei Bajestan [5], studied the impact of main channel wall slope on the sediment

entering lateral intake. The obtained results demonstrated that the change in the main channel wall slope leads to enhancement of flow pattern, in such a way that the amount of sediment entry into the intake was reduced. Moradinejad et al [6] experimentally investigated the sediment control by placing the skimming wall and spillway in the lateral intake span. The results showed that the presence of skimming wall and its combination with spillway led to reduction in the amount of sediment entry into the intake averagely up to 81%, 78% and 76%, for the wall with angle of 10°, 14°and18°, respectively. The preceding studies similar to the present research are as follows: Barkdoll et al. [7] studied the array of submerge vanes, Barkdoll et al. [8] investigated the combination of submerged vanes with skimming wall, Nakato and Odgen [9] focused on the array of submerged vanes and its combination with sill, Barkdoll et al. [2] experimentally scrutinized the array of submerged vanes, their combination with skimming wall and modification of intake span. Nakato et al. [10] used submerged vanes in order to control the sediment in the intake of pumping station located in three Council Bluffs plants, Missouri River. They reported that there has been no need for dredging after 3.5 years of the installation of submerged plates, and the intake has not encountered with any problem regarding the sediments. For resolving sedimentation issue at the intake span located in Cedar River, Iowa, the Wang et al. [11] used submerged vanes system. This system consisted of three rows of plates, which are installed at intake upstream through intake front section. After 1 year, the figures related to the bottom are 0.7m lower than the initial state, and such erosion rate refers to the proper performance of vanes (plates) in controlling the phenomenon. Tan et al. [12] studied the characteristics of the flow and sediment motion around a submerge vane with length of 1 to 4 m, in a wide direct flume. The obtained results demonstrated that the optimal height of the vanes is 2 to 3 times of the vanes bed form and the optimal collision angle for deviating the sediments path is 30°. Ayvaz [13] utilized harmony search algorithm for optimization of the groundwater resource problems. The obtained results showed that this algorithm yielded more proper results, compared to that of other algorithms. Attarzadeh and Ghodsian [14] conducted an experimental study on the efficiency of various systems in combination (with various size) consisted of sill, spillway and submerged vanes for controlling the sediment entry into the lateral intake with 90° angle for intake ratio of 0.12, 0.15 and 0.18. The results ascertained the efficient impact of spillway and submerged vanes on controlling the sediment, and under certain conditions, it was possible to observe efficient close to 100% in removal of inlet sediment from the intake. Fatehi Nobarian [15], in a research entitled “Investigation of the Effect of Velocity on Secondary Currents in Semicircular Channels on Hydraulic Jump Parameters” adopted harmony search algorithm and flow-3d software for studying the jump energy depreciation. Indeed, he studied the application of this metaheuristic algorithm in determining the optimal geometrical sections. Finally, he demonstrated the laudable performance of this algorithm in the field of hydraulic system optimization. The previous studies focused on the application of submerged vanes, spillway and modification of intake span for hindering the sediment entry into the intake. For the first time, the present study aims at controlling the inlet sediment to the lateral intake using parallel skimming walls and employing harmony search algorithm.

3. Methods and materials

3.1. Governing equations derived from experimental method

The experiments and tests are performed at Soil conservation and Watershed Management Research Institute (SCRI) of Tehran, in a flume with 12m in length, 1.5m in width and 0.9m in height incorporating water circulation system. The intaking was accomplished using lateral intake with width of 0.6m, length of 2.6 and angle of 60° relative to the flow direction in the main. The

slope of the main channel was equal to 0.002, with horizontal intake and its balance was aligned with sediment bed of the main channel. The sediments of these experiments were sand with diameter of 1mm, standard deviation of 1.47 and uniformity coefficient of 2.20. Equation (1) and Equation (2) was used for calculating the standard deviation and uniformity coefficient, respectively. Figure 2 depicts accomplished experiments.

$$\sigma_g = (\frac{D_{84}}{D_{16}})^{0.5} = (\frac{1.22}{0.56})^{0.5} = 1.47 \quad (1)$$

$$C_u = \frac{D_{60}}{D_{10}} = \frac{1.1}{0.5} = 2.20 \quad (2)$$

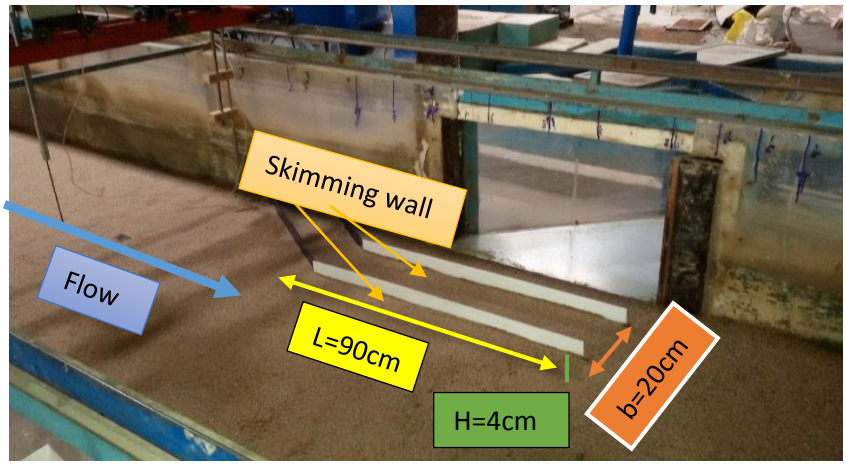

Figure 2. A view of the parallel skimming walls installed at the front of the intake span with a length of 90cm, a height of 4cm at a distance of 20cm

Figure 2 illustrates the parallel skimming walls installed in front of the intake with length of 90cm, height of 4cm and distance of 20cm from each other. It should be noted that the number of parameters contributing to entry of bed load sediments into the intake span is high. For studying the effective parameters, dimensionless numbers were used. After obtaining the data in laboratory and using Buckingham's dimensional analysis, using fitness tool the governing equations were obtained. For skimming wall and in various b modes assuming that we have H=4cm and L=90cm, Equation (3) is as below:

$$C_{s1} = \frac{V}{D^3} = 1.44[Q_R]^{-0.45}[Fr]^{2.16}\left[\frac{b}{H}\right]^{-0.005}\left[\frac{L}{b}\right]^{0.61} \quad (3)$$

Where, C_{S1} denotes deviated sediment ratio, V refers to the volume of inlet sediment into intake, D is flow depth in the main channel, Fr is Froude number of main flow, b refers to distance between the walls, H is plates height in the skimming wall and L refers to the second branch of skimming walls. Moreover, Q_R denotes the intaking ratio yielded by Equation (4), in which Q_L denotes flow discharge for intake channel and Q_m flow discharge for main channel.

$$Q_R = \frac{Q_L}{Q_m} \quad (4)$$

For parallel skimming walls and various θ modes, assuming that we have H=4cm, L=90cm and b=20cm, Equation (5) is as below:

$$C_{s2} = \frac{V}{D^3} = 3.76[Q_R]^{-0.72}[Fr]^{2.46}[\theta]^{0.25} \quad (5)$$

Where, C_{s2} denotes deviated sediment ratio, V refers to the volume of inlet sediment to intake, D is flow depth in the main channel, Q_R is intaking ratio in accordance with Eq. (4), Fr is Froude number of main flow, and θ is angle of second branch of skimming wall with main flow direction. The parameters adopted in laboratory conditions are presented in Table 1.

Table 1. Parameters used in laboratory.

Parameter	L(cm)	b(cm)	H(cm)	θ°	Q_R	Fr
Values	60	10	2	1	0.16	0.30
	75	20	4	15	0.28	0.37
	90	30	6	30	0.35	0.45
	-	-	-	-	0.43	0.56

3.2. Harmony search algorithm method

Over the past four decades, manifold algorithms are devised for solving the various engineering optimization problems. Geem et al. [16] proposed a novel algorithm, called Harmony Search based on the artificial music harmony. As the musicians seeking a mode with best rhythm and ear-catching feature, the optimization algorithms look for the best mode, considering reduction in the cost or surge in the benefit. The optimization process involved in harmony search is accomplished through five phases as below:

Phase 1: Introduction of optimization problem and algorithm parameters

First, the optimization problem is formulated as below:

$$Minimize[f(x)], x_i \in X_i, i = 1,2,...,N \quad (6)$$

Where, $f(x)$ is objective function, x_i is decision-making variable. In the optimization model, the allowed range for decision variable is as follow: $x'_{i\min} < x'_i < x'_{i\max}$, where $x'_{i\min}$ and $x'_{i\max}$ denotes the low bound and high bound of each decision variable. At this stage, a series of parameters specific to the harmony search algorithm, such as Harmony Memory Size (HMS) representing number of solution (result) vectors of the harmony memory, Harmony Memory Consideration Rate (HMCR), Pitch Adjustment Rate (PAR) and maximum number of iterations or stop condition, are taken into account. After obtaining the objective function of each harmony, the harmonies are sorted in the harmony memory.

Phase 2: Generation of initial harmony memory in random manner based on the range of possible values for decision variable.

$$HM = \begin{bmatrix} x_1^1 & x_2^1 & \dots & x_N^1 \\ \vdots & \vdots & \vdots & \vdots \\ x_1^{HMS-1} & x_2^{HMS-1} & \dots & x_N^{HMS-1} \\ x_1^{HMS} & x_2^{HMS} & \dots & x_N^{HMS} \end{bmatrix} \rightarrow \begin{bmatrix} F(x^1) \\ \vdots \\ F(x^{HMS-1}) \\ F(x^{HMS}) \end{bmatrix}$$

Where $F(x^1)$ denotes the value of objective function for the first vector and HM matrix of harmony memory [16].

Phase 3: Generation of a solution or new harmony. To produce a value for i-th variable, first a random number in the range of zero to 1 is generated, then this random number is compared with HMCR and if it is less than HMCR, a value for i-th variable is selected from i-th column of memory matrix, otherwise a random value from the search space is assigned to i-th variable. If a value is selected from memory matrix, then another random number will be produced and it will be compared with PAR. In the case that the random number is less than PAR, this variable which is selected from memory matrix, is transformed into smaller value (using Eq. (7)). For determining the change amount applied on the variable selected from matrix memory, another parameter with bw name (bandiwdth) is defined, and Equation (7) yields the value of new variable:

$$X_{new} = X_{old} + bw \times \varepsilon \qquad (7)$$

In Equation (7), X_{old} denotes the value for the variable stored in the harmony memory and X_{new} emerges as the value of new variable after accomplishment of regulation and transformation operation. In fact, ε is the same as the random number from uniform distribution [-1,1]. That is, it is possible to consider this phase regulation somehow similar to the mutation operator in the genetic algorithm.

Phase 4: Update harmony memory
If the new harmonies are better than the available worst harmonies of the HM, they will be replaced by the new harmonies, and the worse harmony will be expelled from the memory. Otherwise, the algorithm enters another iteration without any substitution.

Phase 5: Check stop criteria
Phases 3 and 4 are iterated until the moment that the stop condition is meet, this condition in the harmony search algorithm is checking of the iteration counts. Of course, it is possible to adjust the stop condition of the algorithm to an optimal value and till finding this value the phases are iterated. So that, the last vector will be the solution of the problem [17].
Figure 3 presents the flowchart of phases 1 through 5.

Advance Researches in Civil Engineering
ISSN: 2645-7229, Vol.4, No.4, pages: 55-70

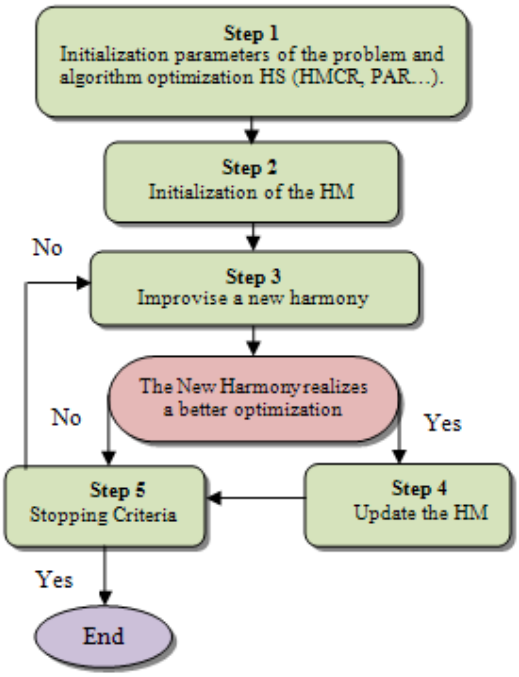

Figure 3. Base flow chart of harmony search (Geem et al., 2001).

Generally, the value of HMCR is assumed to vary between 0.90 to 0.99. Harmony Memory Size ranges between 5 to 50. This parameter is depended on the decision variables count, the greater size of harmony memory, the greater dimension for the problem is expected. So, the main focus is centered on making this parameter smaller. The pitch adjusting rate is assumed to vary between 0.30 to 0.99. It should be noted that, based on the study problem, PAR may be less than the afore-mentioned range [18]. In the present article, for studying how harmony search algorithm operates, a real-world single purpose problem in the field of sediment control in the lateral intakes is studied. This problem is known as the constrained optimization problem, and for defining the problem there is a need for defining the objective function and problem constraints. Controlling the inlet sediment into the lateral intake to reach the mode during which minimum sediment enters into the intake, is considered as the objective function. Table 2 presents the parameters of HS which are employed in this study.

Table 2. Parameters of the Harmonic Search Algorithm used in this research.

Parameter	MaxIt	HMS	nNew	HMCR	PAR
Values	2000	10	10	0.5	0.8

Where, MaxIt refers to the maximum iteration count and nNew represents the new harmonies count. In this study, regarding the objective functions (Eq. 3 and Eq. 5), parameters, including $[Q_R],[Fr],\left[\frac{b}{H}\right],\left[\frac{L}{b}\right],[\theta]$, are used as the autonomous parameters, for which the constraints regarding their application in HS are presented by Table 3.

Advance Researches in Civil Engineering
ISSN: 2645-7229, Vol.4, No.4, pages: 55-70

Table 3. Constraints used for autonomous variables.

Parameter	$[Q_R]$	$[Fr]$	$\left[\frac{b}{H}\right]$	$\left[\frac{L}{b}\right]$	$[\theta]$
Constraints	$0.16 \le Q_R \le 0.43$	$0.30 \le Fr \le 0.56$	$2.5 \le \frac{b}{H} \le 7.5$	$3 \le \frac{L}{b} \le 9$	$1^\circ \le \theta \le 30^\circ$

4. Results and discussion

In this paper, using Equation (3) and Equation (5) along nonlinear fitness method, the experimental data are obtained. For validating the relations, it is essential that statistical index should be used for verifying the closeness extent of the relations to the experimental data. For validating all obtained relations of the present study, the statistical index, such as coefficient of determination (denoted by R2) and Root Mean Square Error (RMSE) are utilized. R^2 denotes the statistical closeness measurement of data to the fitted regression line. The mathematic expression of RMSE is presented by Equation (8):

$$RMSE = [\frac{1}{n}\sum_{i=1}^{n}(C_{s(cal)} - C_{s(obs)})^2]^{0.5} \quad (8)$$

Where, $C_{s(cd)}$ and $C_{s(obs)}$ refer to the calculated and observational value of variable excepted from validation data. n denotes the number of available data. The value of the afore-mentioned index for the best case should be as small as possible and close to zero.

4.1. Validation and determination of optimal points in C_{s1} relation

Equation (3) regarded as one of the objective functions for harmony search algorithm was validated using experimental data and Curve Fitting Toolbox. The results of this validation are presented by Figure 4, where RMSE is equal to 0.0779.

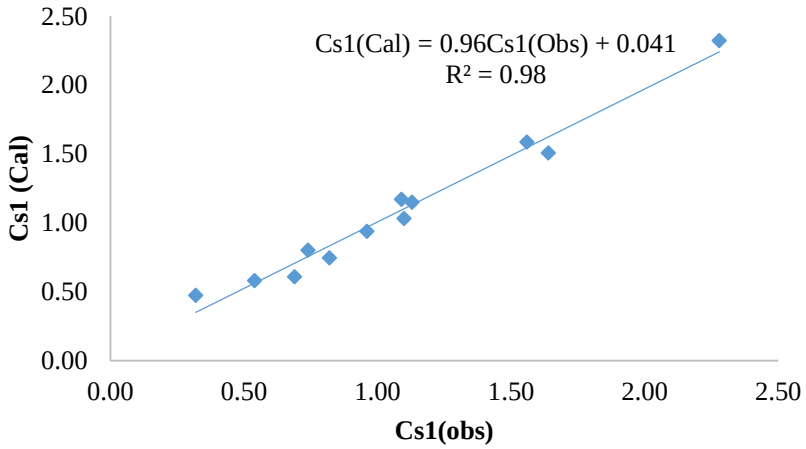

Figure 4. Validation of computational C_{s1} relation with observational data of C_{s1}.

Advance Researches in Civil Engineering
ISSN: 2645-7229, Vol.4, No.4, pages: 55-70

As the main purpose of parallel skimming wall is to reduce the sediment volume entering lateral intake span, so the problem objective function of harmony search algorithm aims at minimizing the sediment amount entry into the lateral intake (C_{s1}). Table 4 presents the minimum, maximum, average values of C_{s1} for laboratory environment, Eq. (3) and harmony search algorithm. The relation between computational C_{s1} and optimized C_{s1} using the data of Table 4 are presented in Figure 5, where RMSE and R^2 is equal to 0.3359 and 0.94, respectively.

Table 4. Minimum, maximum and mean values of C_{s1}-in laboratory, computational relation of C_{s1} and harmony search algorithm.

	Minimum Value ($\min C_{s1}$)	Maximum value ($MaxC_{s1}$)	Average Value ($averageC_{s1}$)
Experimental (Observational)	0.32	2.28	1.07
Eq. (3) (Computational)	0.47	2.32	1.08
Optimization (HSA)	0.42	1.89	0.65

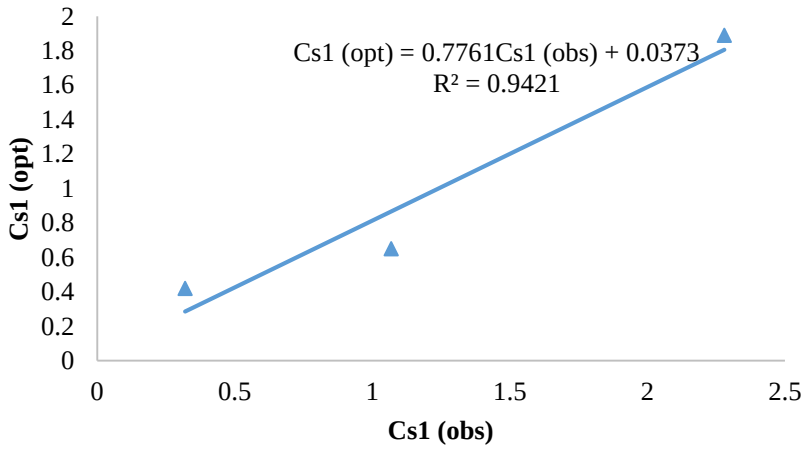

Figure 5. Relation between observational and optimized C_{s1} based on Table 4 data

As seen in Figure 5, there is One-One Relationship between $C_{s1(obs)}$ and $C_{s1(opt)}$ for min, max and average data. Regrading the afore-mentioned points and using harmony search algorithm, the optimized values of autonomous variables of C_{s1} relationship are presented by Table 5.

Table 5. Optimized values of autonomous variables of C_{s1} relation.

Dimensionless Variable	C_{s1}	$[Q_R]$	$[Fr]$	$\left[\frac{b}{H}\right]$	$\left[\frac{L}{b}\right]$
Optimal value (min)	0.42	0.16	0.30	15	2.5
Optimal value (max)	1.89	0.39	0.52	2.30	8.03
Optimal value (average)	0.65	0.25	0.39	13.05	2.81

Using harmony search algorithm, a set of curves are obtained demonstrating the relation of C_{s1} and autonomous variables of Equation (3) for 20000 optimized points (Figures 6, 7, 8, 9.) The colored spectra consisted of dark blue to dark red, in such a way that the warm colors (yellow, orange and red) refer to the optimal values with maximum value. The cold colors (blue and green) are the optimal values with minimum value.

Advance Researches in Civil Engineering
ISSN: 2645-7229, Vol.4, No.4, pages: 55-70

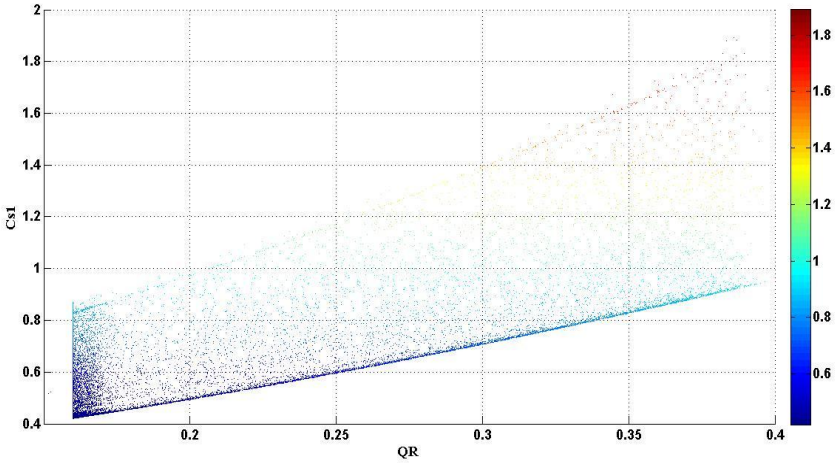

Figure 6. Points optimized for C_{s1} using Q_R dimensionless parameter.

As seen in Figure 6, an increase in Q_R leads to increase in C_{s1}. Majority of the optimal points are located within the range of $0.03 \le Q_R \le 0.10$ and $0.4 \le C_{s1} \le 0.9$. Other points are also optimal, while the number of optimal points at that ranges is less.

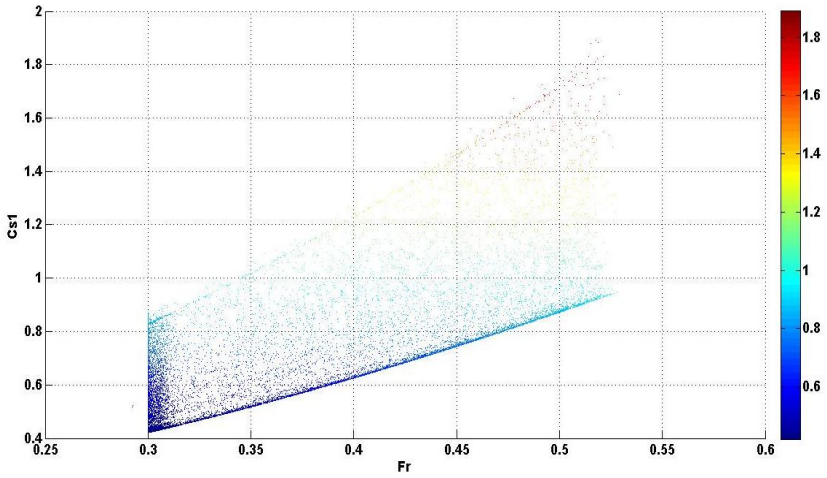

Figure 7. Points optimized for C_{s1} using dimensionless parameter Fr

As seen in Figure 7, an increase in Froude number leads to increase in C_{s1}. The majority of optimal points are located in the range of $0.30 \le Fr \le 0.32$ and $0.4 \le C_{s1} \le 0.8$.

Advance Researches in Civil Engineering
ISSN: 2645-7229, Vol.4, No.4, pages: 55-70

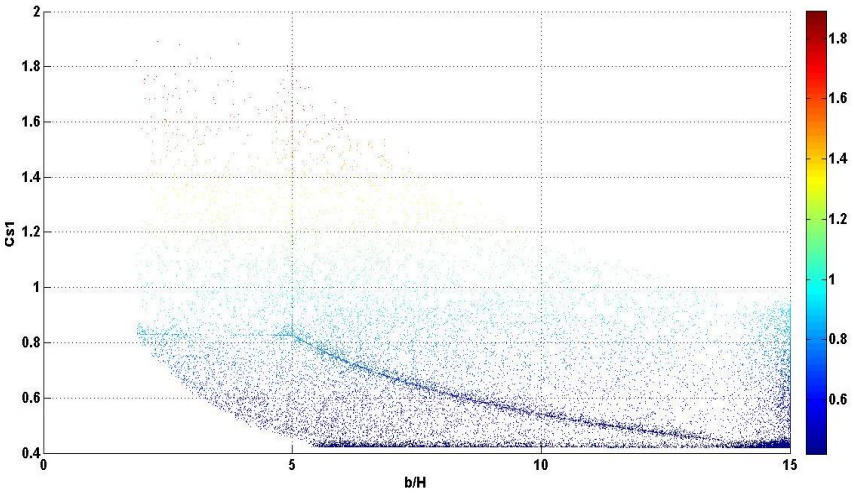

Figure 8. Points optimized for C_{s1} using $\frac{b}{H}$ dimensionless parameter

With regard to Figure 8, an increase $\frac{b}{H}$ value leads to reduction in C_{s1}. The majority of optimal points are located in the range of $5.5 \le \frac{b}{H} \le 15$ and $0.4 \le C_{s1} \le 0.9$.

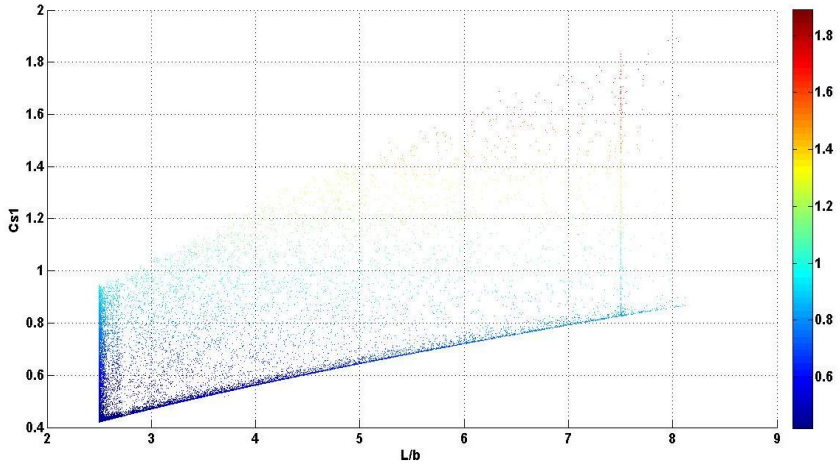

Figure 9. Points optimized for C_{s1} using $\frac{L}{b}$ dimensionless parameter.

As seen in Figure 9, an increase in $\frac{L}{b}$ leads to increase in C_{s1}. The majority of optimal points are found in the range of $2.5 \le Q_R \le 6.0$ and $0.40 \le C_{s1} \le 0.95$.

Advance Researches in Civil Engineering
ISSN: 2645-7229, Vol.4, No.4, pages: 55-70

4.2. Validation and determination of optimal points of C_{s2} relation

Equation (5) is known as one of the objective functions of harmony search algorithm, which was validated using experimental data and Curve Fitting Toolbox™ (Figure 100), where RMSE is equal to 0.0111.

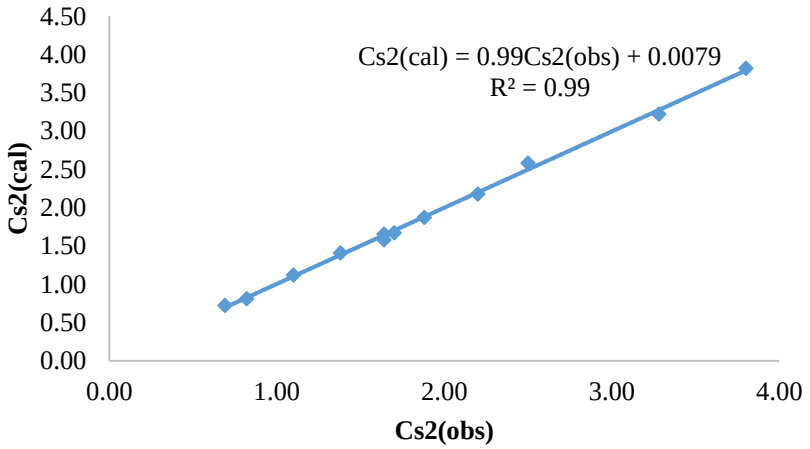

Figure 10. Validation of C_{s2} relation using observational data of C_{s2}

The objective function of harmony search algorithm aims at minimizing the amount of sediment entering lateral intake (C_{s2}). Table 6 presents the minimum, maximum and average values of C_{s2} in laboratory, C_{s2} relation and harmony search algorithm. The relation between observational and optimized C_{s2} based on the data of Table 6, is shown by Figure 11, where RMSE and R^2 is equal to 0.2415 and 0.96, respectively.

Table 6. Minimum, maximum and average values of C_{s2} in laboratory, Eq. (5) and harmony search algorithm

	Minimum Value ($\min C_{s2}$)	Maximum Value ($Max C_{s2}$)	Average Value ($average C_{s2}$)
Experimental (observational)	0.69	3.80	1.88
Eq. (5) (Computational)	0.72	3.82	1.89
Optimization (HSA)	0.72	3.39	1.29

Advance Researches in Civil Engineering
ISSN: 2645-7229, Vol.4, No.4, pages: 55-70

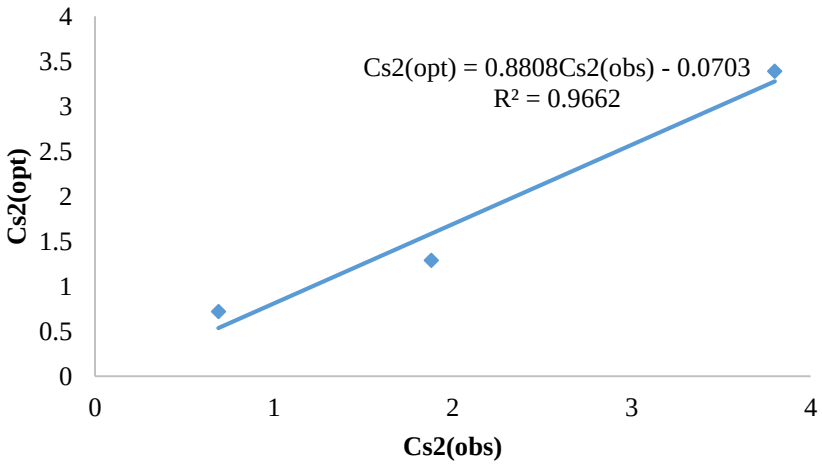

Figure 11. Relation between observational and optimized C_{s2} using data available in Table 6

With regard to the afore-mentioned points and using harmony search algorithm the optimal values for autonomous variables of Equation (5) are presented in Table 7.

Table 7. Optimized values of autonomous variables of Equation (5).

Dimensionless Variable	C_s	$[Q_R]$	$[Fr]$	$[\theta]$
Optimal value (min)	0.72	0.30	0.16	1.00
Optimal value (max)	3.39	0.52	0.39	26.07
Optimal value (average)	1.29	0.44	0.31	1.36

Using harmony search algorithm, a set of curves were obtained demonstrating the relation between C_{s2} and autonomous variables of Eq. (5) for optimized 20000 points (Figures 12, 13, 14).

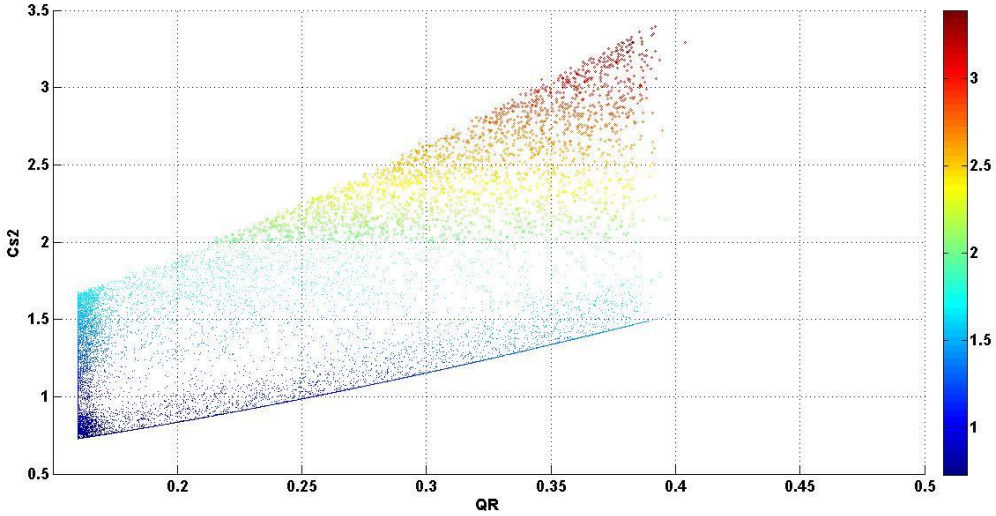

Figure 12. Optimized points for C_{s2} using Q_R dimensionless parameters

In Figure 12, it is evident that the increase in Q_R leads to increase in C_{s2}. The majority of optimal points can be found in the range of $0.16 \le Q_R \le 0.17$ and $0.75 \le C_{s2} \le 1.70$.

Advance Researches in Civil Engineering
ISSN: 2645-7229, Vol.4, No.4, pages: 55-70

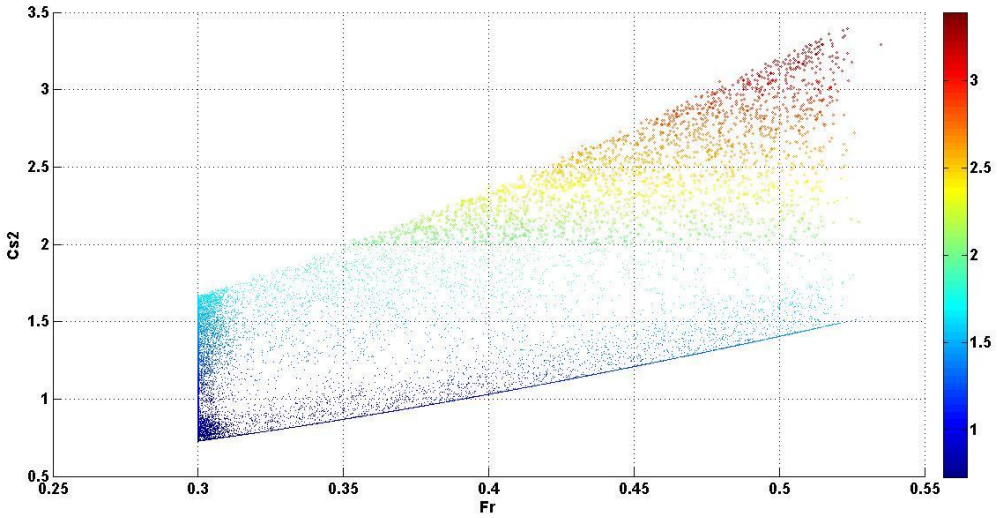

Figure 13. Optimized points for C_{s2} using Fr dimensionless parameter

As seen in Figure 12, an increase in Fr value leads to increase in C_{s2}. The majority of optimal points are located in the range of $0.30 \le Fr \le 0.32$ and $0.75 \le C_{s2} \le 1.60$.

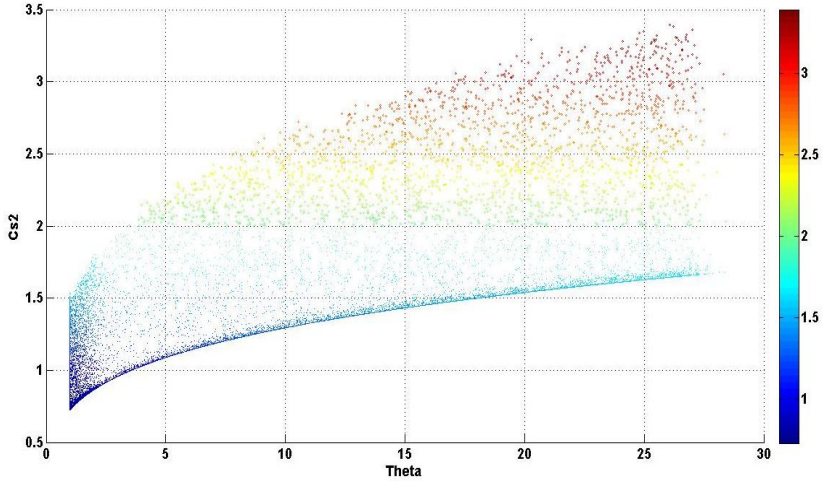

Figure 14. Optimized points for C_{s2} using θ dimensionless parameter

With regard to Figure 14, it can be inferred that an increase in θ value leads to increase in C_{s2}. It should be also note that the majority of optimal points are found in the range of $1 \le \theta \le 3$ and $0.75 \le C_{s2} \le 1.5$.

5. Conclusions

The studies revealed that there is a plethora of optimal points for the certain ranges. The findings of the present research are summarized in following conclusions:

1- In Equation (3) and Equation (5) as the governing equations, C_{s1} and C_{s2} relations is obtained in combination with dimensionless parameters, while in the figures with color spectra, the relation of C_{s1} and C_{s2} is studied, independent from dimensionless parameters, for which there may be difference in terms of sign and exponent (power) value. For instance, in Equation (3), the value for

C_{s1} is the form of combination of Q_R dimensionless figure with negative power, while in Figure 6 where it is studied independently, it holds positive exponent.
2- For governing equation of C_{s1}, the maximum, minimum and average values of optimized C_{s1}, exhibited error rates of 17%, 31% and 39% respectively, compared to the maximum, minimum and average values of observational C_{s1}.
3- For governing equation of C_{s2}, the maximum, minimum and average values of optimized C_{s2}, exhibited error rates of 11%, 4% and 31% relative to the maximum, minimum and average values of observational C_{s2}.
4- In governing equation of C_{s1}, regarding the great value of exponents, Froude number with power of 2.16, is the most effective dimensionless parameter on C_{s1} value, while $\left[\frac{b}{H}\right]$ value with exponent of -0.005 showed the lowest effect on the value of C_{s1}.
5- In governing equations of C_{s2}, regarding the great value of exponents, Froude number with power of 2.46, is taken into account as the most effective dimensionless parameter on the value of C_{s2}, and $[\theta]$value with exponent of 0.25 showed the lowest impact on the C_{s2} value.

6- In governing equation of C_{s1}, the relations are validated based on the experimental data, during which the sensitivity analysis revealed that the exclusion of dimensionless parameters from the governing equation, including $[Q_R]$ and $\left[\frac{b}{H}\right]$, the value of R^2 and RMSE will be equal to 0.97 and 0.0869, respectively, which do not differ significantly with governing equation of C_{s1} (The error rate for R and RMSE is equal to 1% and 11%, respectively).
7- In governing equation of C_{s2}, the validation was performed based on the experimental data, where R^2 and RMSE was equal to 0.99 and 0.0111, respectively.

6. References

1- Neary, V. S., and Odgaard, A. J. 1993, **Three-dimensional flow structure at open channel diversions**, J. Hydraulic. Eng., ASCE, 119, 11, 1224–1230.
2- Barkdoll, D., Ettema, R. and Odgaard. A.J. 1999, **Sediment control at lateral diversions: limits and enhancement to vane use**, Journal of Hydraulic Engineering, 125, 8.
3- Odgaard, A. J. and Wang, Y., 1991, **Sediment management with submerged vanes I**. theory. Hydraulic Engineering, 117, 3, 267-283.
4- Abbasi, A.A. 2004, **Experimental Study on Controlling inlet Sediment to Lateral Intakes in Direct paths (PhD Dissertation)**, Faculty of Engineering, Tarbiat Modares University, p.192
5- Seyedian, M. and Shafaei Bajestan, M. 2011, **Comparison of Suspended Load Delivered Into the Intake by Changing the Canal Side Angle from Perpendicular to 45 Degrees**, Journal of Water and Soil, 24, 5, Nov-Des 2010, 985-994.
6- Moradinejad, A., Haghiabi, A. H., Saneie, M., Yonesi, H., 2017, **Investigating the Effect of Skimming Wall on Controlling the Sediment Entrance at Lateral Intakes**, Water Science & Technology, Water Supply, 17, 4, 1121-1132.
7- Barkdoll, B. D. and Hagen, B.L. and Odgaard, A.J. 1995, **Sediment exclusion at hydropower intakes using submerged vanes**, Proc. waterpower, ASCE, 1, 3, 892-908.
8-Barkdoll, B. D., Ettema, R. and Thou, J. 1997, **Sediment Control at Riverside Water Intakes**, Proc. of the International Joint Power Generation Conference, Denver, U.S.A., 227-232.
9-Nakato, T. and Odgen, F. L. 1998, **Sediment Control at Water intakes along Sand Bed Rivers**, Journal of Hydraulic Engineering, ASCE, 116, 1, 119-128.

10- Nakato, T., Kennedy, J.F. and Bauerly, D. 1990, **Pump – station Intake – shoaling control with submerged vanes**. Journal of Hydraulic Engineering, ASCE, 116, 1, 119-128.
11- Wang, Y., Odgaard, J., Melville, W., Jain, C. 1996, **Sediment control at water intakes**, Journal Of Hydraulic Engineering, 122, 6., 353-356.
12- Tan, S.K.,Yu, G., Lim, S.Y. and Ong, M. C. 2005, **Flow Structure and Sediment Motion around Submerged vanes in open channel**, JWPCOE, 131, 3.
13- Ayvaz, M. and Tamer. 2010, **Solution of groundwater management problem using harmony search algorithm**, Stud. Comput. Intell. 270, 111-122.
14- Attarzadeh, A. and Ghodsian, M. 2018, **Study on Flow Separation Width and Control Over the Sediments in Various Systems of Lateral Intake**. 17th National Hydraulic Conference, Shahr Kord, Iran.
15- Fatehi-Nobarian, B., Panahi, Razieh., Nourani, Vahid. 2022, **Investigation of the Effect of Velocity on Secondary Currents in Semicircular Channels on Hydraulic Jump Parameters**. Iranian Journal of Science and Technology, Transactions of Civil Engineering, https://doi.org/10.1007/s40996-021-00800-x 46(4), 3351-3359.
16- Geem, Z.W., Kim, J.K., Loganathan, G.V. 2001, **A new heuristic optimization algorithm**: **harmony search**, simulation.
17- Janat Rostami, S., Kholghi, M. and Bozorg Hadad, O. 2010. **Management of Reservoir Operation System Using Improved Harmony Search Algorithm. Water and Soil Science**, Volume 20, Issue 3, Autumn 2010, 61-71
18- Mahdavi, M., Fesanghary. M., Damangir, E, 2007, **An improved harmony search algorithm for solving optimization problems**, Applied mathematics and computation, 188, 1567-1579.